Proceedings of the 17th World Congress
The International Federation of Automatic Control
Seoul, Korea, July 6-11, 2008

Non-linear Identification and Analysis of a HEUI System

Jui-Jung Liu * Ya-Wei Lee**
Shih-Yen Yang Chiz-Chung Cheng*****

** Department of Information and Electronic Commerce, Kainan University, Taoyuan, Taiwan (Tel: +886-3-3412500-2601; e-mail: jjliu@ mail.knu.edu.tw).*
*** Ordnance Readiness and Development Center, Nantou, Taiwan (Tel: +886-2-27913360; e-mail:d91522007@ ntu.edu.tw)*
****Electrical Engineering Department, Lee-Ming Institute of Technology, Taipei, Taiwan (e-mail: abcd0428@ms23.hinet.net)*

Abstract: This study presents the estimation of a nonlinear autoregressive moving average with exogenous inputs (NARMAX) model of a novel hydraulically actuated electronic unit injection (HEUI) system. The injection pressure-fuel rate relationship is detected to understand the HEUI system and its effects on engine performance. The dynamics of causation is first investigated in the time domain to estimate the non-linear models. Further validation is then done using model predicted output, correlation tests and cross-validation tests.

1. INTRODUCTION

Many turbo charged diesel engine dynamics studies have been carried out using various approaches and the modelling of such engines is an issue of some importance (Evans et al., 1998; Kimmich et al., 2005; Carlucci et al., 2006). These investigations may be classified into time domain and frequency domain methods which involve numerical integration of motions, neuro fuzzy optimization techniques and experimental estimation (Xu et al., 2002; Galindo et al., 2005). Gangopadhyay and Meck (1997) developed a model of a central fuel injected natural gas engine with transmission and carried out linear system identification to identify key model parameters that lead to automated identification of transmission dynamics. Hafner et al. (1999) presented an approach for model based control of combustion engine exhaust. Bustamante et al. (2000) developed a throttle control system for a small V-twin engine used in a hybrid AC power generation system that incorporated a wind turbine and an internal combustion engine-generator combination. Frequency domain methods are quite efficient for performing stochastic analysis. However, prior to frequency domain analysis, a Fast Fourier Transform (FFT) is usually employed to transform the time domain signal to a spectrum distribution on a linear frequency domain (Kadjoudj et al., 2001; McNames et al. 2002, Haruna et al., 2003). Therefore, the dynamic characteristics of a nonlinear system could be shown by the power spectral density (PSD) derived from experimental data. Actually, cross modulation, desensitization, and gain compression/expansion which are generated within frequencies may exist simultaneously, and these cause nonlinear phenomena in the frequency domain. Analysis of non-linear systems in the frequency domain is advantageous as integral equations which relate the input-output in the time domain become algebraic in the frequency domain. The present study is based on the NARMAX (Non-linear Auto-Regressive Moving Average with eXogenous inputs) (Fung et al., 2003; Ge et al., 2004; Billings and Wei, 2005; Wei et al., 2005) modelling technique to build a model which can predict the outputs accurately. Thereafter, by applying a recursive probing algorithm to NARMAX models, it is possible to obtain the non-linear frequency response functions of real systems so that the analysis and application of non-linear transfer functions become more practical.

2. SYSTEM DESCRIPTION AND EXPERIMENTAL DESIGN

The power pack used in the study consists of an electronically controlled high power-density Caterpillar C9 diesel engine designed in 2001, coupled to an automatic transmission with a TC-541 torque converter, a transfer box, and a cooling system (Fig. 1). An engine control module (ECM) named ADEM III is equipped on the engine for central fuel control estimation and providing self-diagnosis nodes and interface of transmission control.

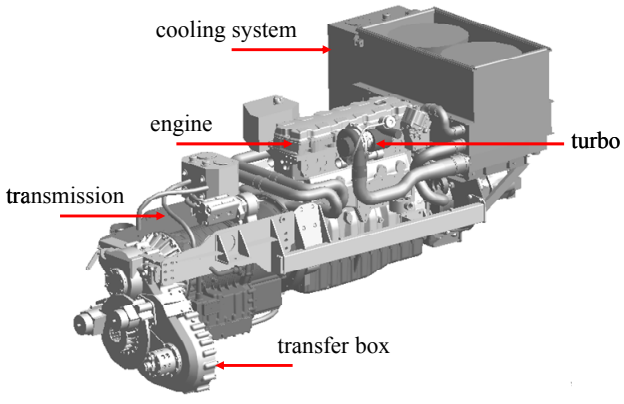

Fig. 1. The power pack system

One of the biggest evolutionary steps of diesel injection technology for this engine is the hydraulically actuated electronic unit injection (HEUI) system (Fig. 2). Until its inception, fuel pressurization for injection has been accomplished using camshafts. Whether engine mounted or used in an injection pump, cam operated pumping, plungers have been the traditional mechanism to supply injection force. However, HEUI unconventionally uses hydraulic force to supply injection pressure. An engine driven oil pump is used to pressurize fuel inside a uniquely designed injector. HEUI technology has also enabled the integration of valve-train operation into this high-pressure actuation system. Electro-hydraulic operation of intake and exhaust valves have demonstrated the tremendous advantages of variable valve timing, valve lift, and duration unencumbered by the fixed geometry of the camshaft. In order to reveal the effect of injection pressure on fuel rate, the model need to be built.

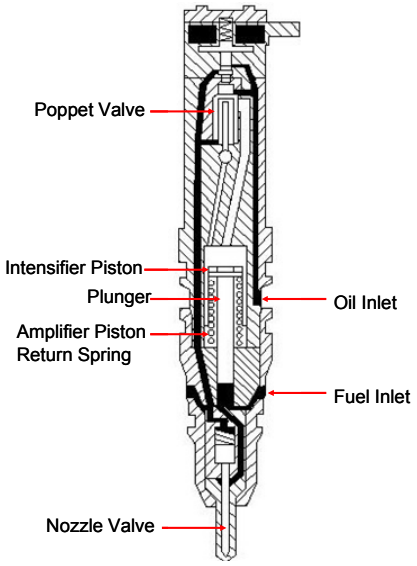

Fig. 2. The schematic HEUI system

The specifications of the engine are given in Table 1. The coupled transmission belongs to the type of off-road wide-ratio Allison HD4560P, which is a six forward plus one reverse speed automatic transmission having differentials and final drives on both the rear and front cabins. The transfer box is developed with a allowable maximum torque of 15000Nm, and a reduction ratio of 1.17. In order to completely identify the dynamics of the HEUI, wide range of fuel rate, varying from 0~80 L/H, is adopted to run the engine on a free-load condition. The engine need to be run for at least 60 minutes before sampling, and the samples are selected at a specific duration of 30 seconds (sampling rate is 40Hz). Together with digital control and data acquisition systems, this engine testing system can be easily used for simple overhaul test applications through high level research and development.

3. RESULTS AND DICUSSIONS

The HEUI system is identified by the time series of injection pressure and fuel rate. The input data representing the injection pressure is given as multi-sinusoidal waves, while the corresponding output data is the fuel rate. These are shown in Fig. 3.

Table 1. Specifications of Caterpillar C9 heavy-duty diesel engine

Cylinders	In-Line 6
Bore/Stroke	112mm / 149mm
Displacement	8.8 L
Dry Weight	776kg
Aspiration	Turbocharged
Compression Ratio	15.0~17.0:1
Weight	680 kg
Horsepower	285~400 HP @ 2100 rpm
Torque	1206~1560 Nm @ 1400 rpm

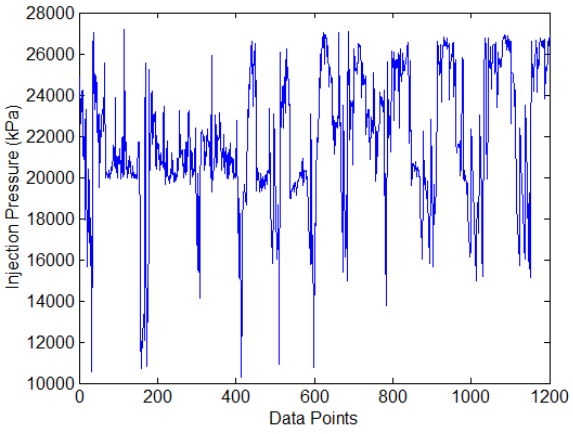

(a)

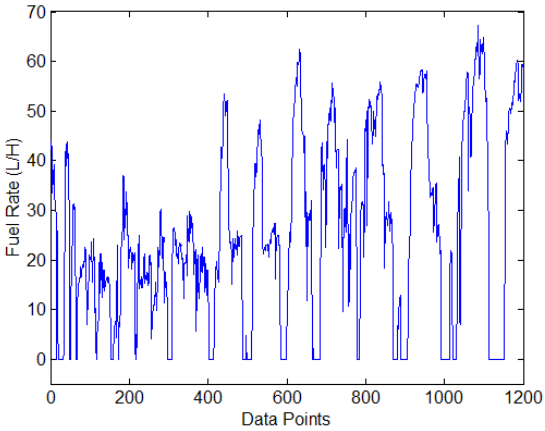

(b)

Fig. 3. I/O signals taken from the 1001st to 2200th samples: (a) injection pressure is for input, and (b) fuel rate is for output

The prediction model is listed in Table 2, where y(k-1), u(k-1) and constant terms are evaluated as the three most important terms.

Table 2. Quadratic injection pressure-fuel rate NARX model

Term	Coefficient	ERR_i
y(k-1)	+0.67421	0.9937
u(k-1)	+0.86549e+2	0.8036e-3
constant	+0.10221e+5	0.4983e-3
y(k-1)u(k-2)	-0.53194e-2	0.1991e-3
y(k-2)y(k-2)	+0.35097e-5	0.5566e-4
u(k-1)u(k-2)	-0.23182e+2	0.4899e-4
y(k-2)	-0.31181	0.2458e-4
u(k-2)u(k-2)	+0.10661e+2	0.2364e-4
y(k-2)u(k-1)	+0.12970e-1	0.1153e-4
u(k-1)u(k-1)	+0.66372e+1	0.1032e-4

In Fig. 4, comparisons between the measured and predicted outputs are reported.

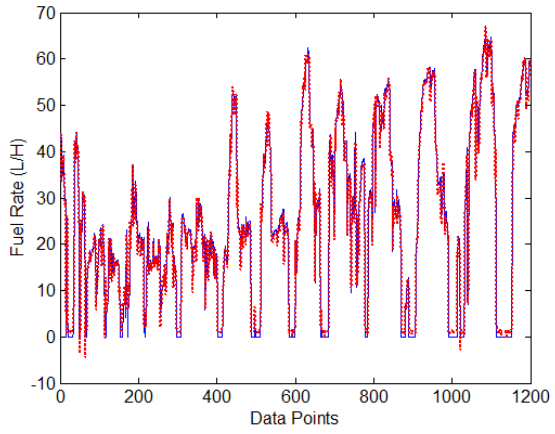

Fig. 4. Comparison of measured (solid line) and predicted (dotted line) fuel rate

The simulated time series approximates the experimental data satisfactorily and about 93% comparisons are within a deviation of ±10% relative error (Fig. 5). The correlation tests of inputs and residuals for injection pressure-fuel rate model are shown in Figure 6 and they are all within the confident limits of 95%. As the model predicts quite well and has acceptable correlation tests then the model can adequately represent the system dynamics.

It is realized that mechanically governed fuel systems have several handicaps. First, mechanical systems pressurize fuel by either an engine or an injection pump camshafts. These systems could not vary injection timing or alter fuel rate with the flexibility needed for emission reductions. Engine operating conditions such as load, coolant and air inlet temperature, inlet boost pressure, vehicle speed, atmospheric pressure and other factors require unique injection timing and rate control to obtain optimum performance, fuel economy and emission reduction. Most critically, these mechanically actuated fuel systems could not adequately pressurize fuel at low engine speeds to obtain better possible atomization and distribution of fuel in the combustion chamber. Since fuel plunger velocities are dependent on engine speed, at low rpm, plunger speeds are proportionally slower, hence preventing high pressurization. The HEUI system develops peak injection pressure independent of engine speed. This means that maximum spray-in pressure is available whether the engine is operating at high or low rpm. By experimental analysis, this feature is demonstrated in Fig. 7. Therefore, during hard acceleration or sudden load changes at low speeds, the system can instantly adjust fuel pressurization to meet the requirements for good performance while minimizing emissions. Electronic control of injection timing and fuel rate mean these events are adjustable, taking into account vehicle and engine operating conditions for lower emissions and peak performance.

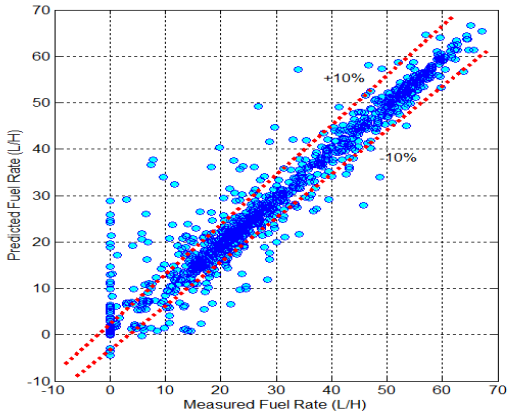

Fig. 5. Cross-validation of measured and predicted fuel rate

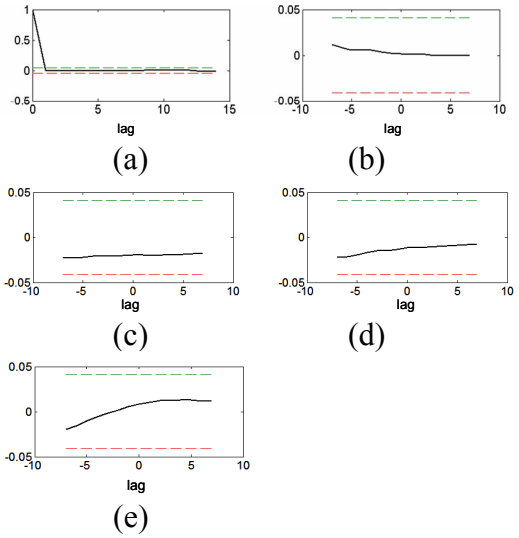

Fig. 6. Correlation tests of inputs and residuals for injection pressure-fuel rate model

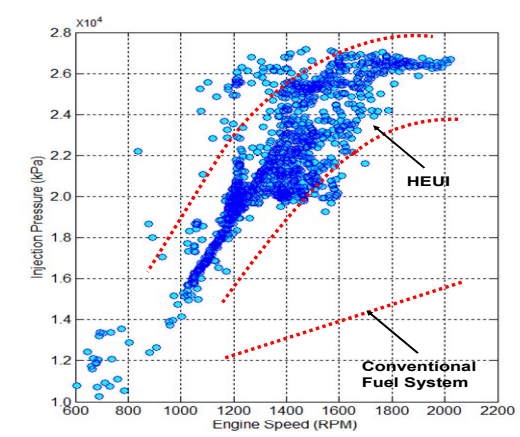

Fig. 7. Comparison of engine performance between conventional fuel system and HEUI system

The model was illustrated on a range of signals and shown to follow the output behaviour of the engine extremely well. However, the physical interpretability of the model is deficient. This is due to inherent problems with discrete time estimation using band-limited input signals and also to the great variability of the model parameters when different nonlinear terms are included. Nevertheless, such a model represented as a difference equation could provide the basis for a global nonlinear controller of the fuel injection system.

In time domain modelling, 1200 pairs of input and output time histories from measurements are used with a sampling rate of 40Hz. Through the GFRF approach, these data belonging to power series can be converted into frequency domain to show real system dynamics. The interpretation of linear and non-linear effects in the frequency domain are illustrated by the GFRFs computed using the models in Table 2.

By equating the $e^{j2\pi f_1 t}$ harmonics, the first-order GFRF obtained from (1) is

$$H_1(f_1) = \frac{+86.549\exp(-j2\pi f_1)}{1-0.67421\exp(-j2\pi f_1)+0.31181\exp(-j2\pi(2f_1))} \quad (1)$$

The linear gain and phase plot are shown in Fig. 8. Two resonant peaks are appeared at normalized frequencies of 0.14 and 0.36 (i.e. f_1=0.14 and f_1=0.36).

To compute the second-order GFRF, both $e^{j2\pi f_1 t}$ and $e^{j2\pi(f_1+f_2)t}$ harmonics need to be kept. The second-order GFRF can be obtained as

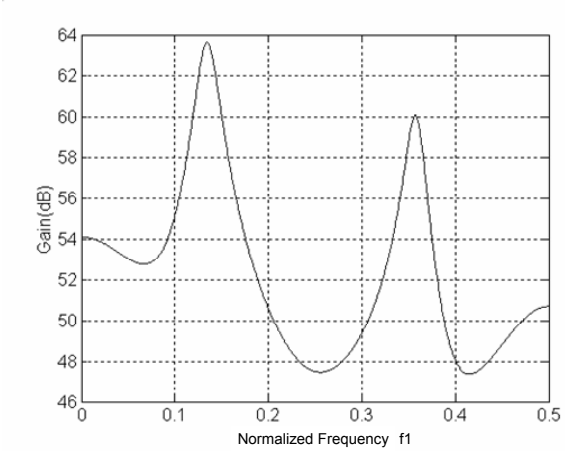

(a)

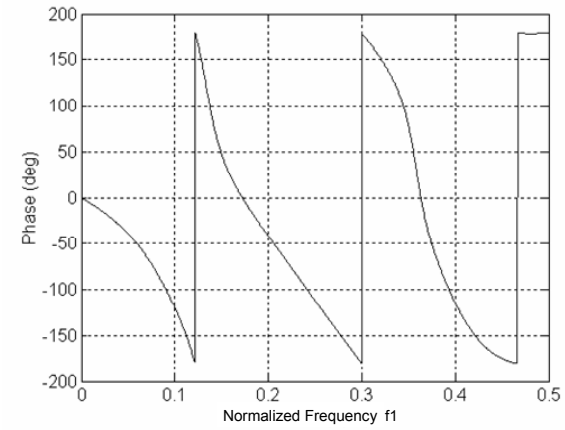

(b)

Fig. 8. (a) The first-order GFRF and (b) phase angle of fuel rate-injection actuation pressure model

$$H_2(f_1,f_2) = \frac{\begin{array}{l} -0.23182\times10^{2}\left(\exp\left(-j2\pi\left(f_1+2f_2\right)\right)+\exp\left(-j2\pi\left(2f_1+f_2\right)\right)\right) \\ +2\times0.10661\times10^{2}\exp\left(-j2\pi\left(2f_1+2f_2\right)\right) \\ +2\times0.66372\times10^{1}\exp\left(-j2\pi\left(f_1+f_2\right)\right) \\ +H_1(f_1)\begin{pmatrix} -0.53194\times10^{-2}\left(\exp\left(-j2\pi\left(f_1+2f_2\right)\right)+\exp\left(-j2\pi\left(2f_1+f_2\right)\right)\right) \\ +0.12970\times10^{-1}\left(\exp\left(-j2\pi\left(2f_1+f_2\right)\right)+\exp\left(-j2\pi\left(f_1+2f_2\right)\right)\right) \end{pmatrix} \\ +H_1(f_1)H_1(f_1)\left(0.35097\times10^{-1}\left(\exp\left(-j2\pi\left(2f_1+2f_2\right)\right)\right)\right) \end{array}}{2!\left(1-0.6742\exp\left(-j2\pi\left(f_1+f_2\right)\right)+0.31181\exp\left(-j2\pi\left(2f_1+2f_2\right)\right)\right)} \quad (2)$$

It is obvious that $H_1(f_1)$ corresponds to the linear transfer function of injection pressure-fuel rate system and illustrates no information about the non-linear effects. On the other hand, $H_2(f_1,f_2)$ involved the linear and quadratic non-linearity relates directly to the non-linearity. Indeed, the non-linear phenomena can be analyzed through the frequency responding surface and iso-curves of $H_2(f_1,f_2)$ (Fig. 9).

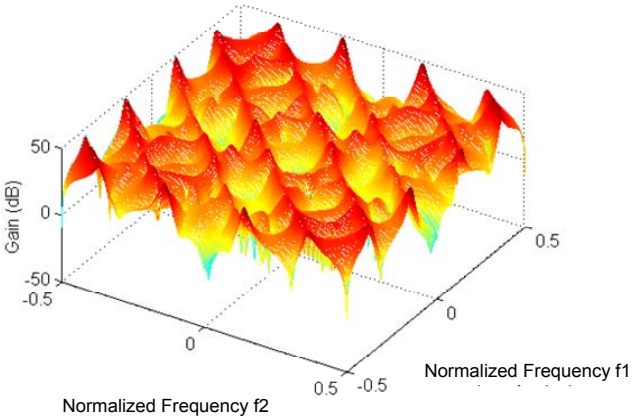

(a)

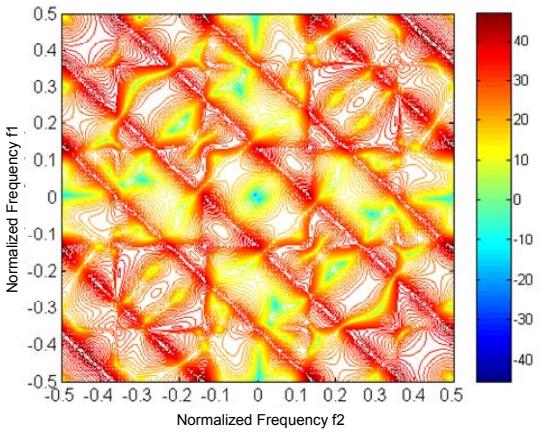

(b)

Fig. 9. The second-order GFRF of fuel rate-injection actuation pressure model: (a) frequency responding surface, and (b) iso-curves

Strong amplifications, f_1=±0.14, f_2=±0.14, f_1=±0.36, f_2=±0.36, f_1+f_2=±0.14, and f_1+f_2=±0.36 can be observed in Fig. 9, which are related to primary resonance effect. Multiplying the sampling rate, the real resonances can be determined at ±5.6Hz and ±14.4Hz. Other phenomena such as resonance in combination can also be demonstrated by this figure. Due to cross modulation, the non-linear gain is generally smaller than the linear gain. The maximum value of linear gain is 63.5dB and non-linear gain is 50dB. From $H_1(f_1)$ and $H_2(f_1,f_2)$ analysis, it can be concluded that non-linear phenomenon does not bring new harmonics but modifies the linear response.

The functions f_1+f_2=±0.14 and f_1+f_2=±0.36 can be seen as forms of resonance behaviours, where energy at the input frequencies f_1 and f_2, which satisfy f_1+f_2=±0.14 and f_1+f_2=±0.36 are transferred to ±5.6Hz and ±14.4Hz frequencies respectively. In contrast, the functions f_1=±0.14 and f_2=±0.36 can be seen as a release of energy phenomena, in which input frequency components close to ±5.6Hz and ±14.4Hz are amplified by the system and transferred to frequency components in the output other than ±5.6Hz and ±14.4Hz. The low frequency components in this case correspond to long time events, which are transferred by non-linear effects to higher frequency or shorter time events.

The causal relation between injection pressure and fuel rate has been identified by both time and frequency domains. Furthermore, the energy transfer between these two parameters could be detected. It is important to note that even though the models analyzed are different in terms of model structure, all the models generated give almost identical GFRFs. That is, the frequency domain response functions are seen as invariants of a non-linear system.

4. CONCLUSION

It is possible to apply the NARMAX approach to multi-dimensional mechanical systems. Using this approach, the model can accurately describe the non-linear features embedded in the system. The novelty of the current results relates to the nonlinear frequency domain analysis performed using the GFRFs. Non-linear resonances are occurred at ±5.6Hz and ±14.4Hz for injection pressure-fuel rate system. The GFRFs reveal that for the fuel system application, nonlinear couplings between input harmonic components take place at low frequency and also on particular lines of frequency.

REFERENCES

Carlucci, A.P., A. Ficarella and D. Laforgia (2006). Control of the combustion behavior in a diesel engine using early injection and gas addition. *Applied Thermal Engineering*, **26**, 2279-2286.

Kimmich, F., A. Schwarte and R. Isermann (2005). Fault detection for modern diesel engines using signal and process model-based methods. *Control Engineering Practices*, **13**, 189-203.

Evans, C., D. Rees and D. Hill (1998). Frequency-domain identification of gas turbine dynamics. *IEEE Transactions on Control Systems Technology*, **6 (5)**, 651-662.

Galindo, J., J.M. Lujan, J.R. Serrano and L. Hernadez (2005). Combustion simulation of Turbocharger HSDI Diesel engines during transient operation using neural networks. *Applied Thermal Engineering*, **25**, 877-898.

Xu, K., L.C. Tang, M. Xie, , S.L. Ho and M.L. Zhu (2002). Fuzzy assessment of FMEA for eigine systems. *Reliability Engineering and System Safety*, **75**, 17-29.

Gangopadhyay, A., P. Meckl (1997). Modeling, validation and system identification of a natural gas engine. *Proceedings of the American Control Conference*, **1**, 294-298.

Hafner, M., M. Schueler and O. Nelles (1999). Dynamical identification and control of combustion engine exhaust. *Proceedings of the American Control Conference*, **1**, 222-226.

Bustamante, J., B. Diong and R. Wicker (2000). System identification and control design of an alternative fuel engine for hybrid power generation. *Proceedings of the Intersociety Energy Conversion Engineering Conference*, **1**, 329-339.

Royzman, V.P. and G. Fomenchenko (2000). Dynamic characteristics identification of aircraft engine by method of trial parameters. *The International Society for Optical Engineering*, **4062**, 885-890.

Kadjoudj, M., R. Abdessemed, N. Golea and M.E. Benbouzid (2001). Adaptive fuzzy logic control for high performance PM synchronous drives, *Electric Power Components and Systems*, **29(9)**, 789-807.

McNames, J., C. Crespo, M. Aboy, J. Bassale, L. Jenkins and B. Goldstein (2002). Harmonic spectrogram for the analysis of semi-periodic physiologic signals, *Annual International Conference of the IEEE Engineering in Medicine and Biology - Proceedings*, **1**, 143-144.

Haruna, T., Y. Morikawa, S. Fujimoto and T. Shibata (2003). Electrochemical noise analysis for estimation of corrosion rate of carbon steel in bicarbonate solution, *Corrosion Science*, **45(9)**, 2093-2104.

Fung, E., M.P. Mignolet, Y.K. Wong and H.F. Ho (2003). Modelling and prediction of machining errors using ARMAX and NARMAX structures, *Applied Mathematical Modelling*, **27(8)**, 611-627.

Ge, S. S., J. Zhang and T. H. Lee (2004). Adaptive MNN control for a class of non-affine NARMAX systems with disturbances, *Systems and Control Letters*, **53(1)**, 1-12.

Billings, S. A. and H.L. Wei (2005). The wavelet-NARMAX representation: A hybrid model structure combining polynomial models with multiresolution wavelet decompositions. *International Journal of Systems Science*, **36(3)**, 137-152.

Liu, J. J., Y.W. Lee, F.C. Wang, R. Uppala and P.H. Chen (2006). Time and frequency domain identification and analysis of a permanent magnet synchronous servo motor. *Journal of the Chinese Institute of Engineers*, **29(4)**, 683-695.

Lee, Y.W., T.L. Chang, F.H. Ko S.H., Chang and C.C. Chen (2007). Experimental and theoretical analysis of microjet droplet behavior. *Microelectronic Engineering*, **84 (5-8)**, 2007, 1770-1774.